Pyrolysis characteristics of cathode from spent lithium-ion batteries using advanced TG-FTIR-GC/MS analysis

Pyrolysis characteristics of cathode from spent lithium-ion batteries using advanced TG-FTIR-GC/MS analysis

Shaoqi Yu[1] · Jingjing Xiong[1] · Daidai Wu[2] · Xiaoshu Lü[3,4] · Zhitong Yao[1] · Shaodan Xu[1] · Junhong Tang[1]

Abstract

Thermal treatment offers an alternative method for the separation of Al foil and cathode materials during spent lithium-ion batteries (LIBs) recycling. In this work, the pyrolysis behavior of cathode from spent LIBs was investigated using advanced thermogravimetric Fourier transformed infrared spectroscopy coupled with gas chromatography-mass spectrometer (TG-FTIR-GC/MS) method. The fate of fluorine present in spent batteries was probed as well. TG analysis showed that the cathode decomposition displayed a three-stage process. The temperatures of maximum mass loss rate were located at 470 °C and 599 °C, respectively. FTIR analysis revealed that the release of CO_2 increased as the temperature rose from 195 to 928 °C. However, the evolution of H_2O showed a decreasing trend when the temperature increased to above 599 °C. The release of fluoride derivatives also exhibited a decreasing trend, and they were not detected after temperatures increasing to above 470 °C. GC-MS analysis indicated that the release of H_2O and CO displayed a similar trend, with larger releasing intensity at the first two stages. The evolution of 1,4-difluorobenzene and 1,3,5-trifluorobenzene also displayed a similar trend—larger releasing intensity at the first two stages. However, the release of CO_2 showed a different trend, with the largest release intensity at the third stage, as did the release of 1,2,4-trifluorobenzene, with the release mainly focused at the temperature of 300–400 °C. The release intensities of 1,2,4-trifluorobenzene and 1,3,5-trifluorobenzene were comparable, although smaller than that of 1,4-difluorobenzene. This study will offer practical support for the large-scale recycling of spent LIBs.

Keywords Electronic waste · Lithium-ion batteries · Cathode · Pyrolysis · Polyvinylidene fluoride binder

Introduction

The rapid growth in the production and consumption of lithium-ion batteries (LIBs) for portable electronic devices and electric vehicles has resulted in a large quantity of spent LIBs (Sun et al. 2018; Tran et al. 2019; Wang et al. 2019a; Xiao et al. 2020; Zeng and Li 2014). More than 11 million tonnes of spent LIB packs are expected to be discarded by 2030, worldwide—500,000 metric tonnes from China alone, by 2020. As we all know, a considerable portion of valuable metals, such as Li, Co, Cu, and Al are reserved within these spent LIBs. In view of their negative effects of spent LIBs on the environment and the considerable amounts of valuable metals reserved in them, it is highly desirable and beneficial to recycle this waste (Winslow et al. 2018; Zhang et al. 2018d). However, such recycling is still a challenge, and only about 5% of the spent LIBs are in fact recycled (Natarajan and Aravindan 2018). Recently, many advanced technologies, such as hydrometallurgy, pyrometallurgy, and bio-metallurgy, have been developed for recycling spent LIBs (Liu et al. 2019; Zhang et al. 2018c; Zhao et al. 2019). Carbon black contained in spent LIBs can be separated through mechanical treatment because of the low adhesion between carbon black and copper foil. However, the Al foil and cathode materials are difficult to separate because they are firmly adhered by polyvinylidene

✉ Zhitong Yao
sxyzt@126.com

✉ Junhong Tang
tangjunhong@hdu.edu.cn

[1] College of Materials and Environmental Engineering, Hangzhou Dianzi University, Hangzhou 310018, China

[2] Guangzhou Institute of Energy Conversion, Chinese Academy of Sciences, Guangzhou 510640, China

[3] Department of Electrical Engineering and Energy Technology, University of Vaasa, FIN-65101 Vaasa, Finland

[4] Department of Civil Engineering, Aalto University, FIN-02130 Espoo, Finland

fluoride (*PVDF*) binder (Wang et al. 2019b; Zeng and Li 2014; Zhang et al. 2018a). A common method of detaching cathode materials from Al foil consists of dissolving Al foil with acidic or alkaline solutions (Chen and Zhou 2014; Gao et al. 2018). The dissolved metals can be further refined by extraction or precipitation processes. However, refractory wastewater will be generated by this method. *PVDF* can be dissolved using organic solvents (e.g., ionic liquid, *N*-methyl-2-pyrrolidone, *N*,*N*-dimethylformamide) according to the "like dissolves like" rule (Duan et al. 2018; Natarajan and Aravindan 2018; Zeng and Li 2014). This method is efficient, but the use of volatile or expensive solvents will not only increase the recycling cost but also pose a risk to workers in the recycling facilities. *PVDF* can also be partially ruptured by oxidants, such as Fenton regents (He et al. 2017). However, wastewater containing impurity ions will be generated as well. Decomposing *PVDF* using thermal treatment offers advantages of high efficiency and simple operation (Cheng et al. 2019; Qi et al. 2019; Wang et al. 2018). Wang et al. (2019b) used molten salt technology to decompose *PVDF*. The maximum detaching rate of cathode material reached 99.8 wt.%. Zhang et al. (2018a, 2018b, 2018c, 2019) and Wang et al. (2018) applied pyrolysis treatment to remove *PVDF*. The recovery rate of cathode materials reached 98.23% under optimal conditions. Xiao et al. (2017) used vacuum pyrolysis to treat cathode material, and lithium carbonate was recovered, although it is worth noting that the fluorine present in *PVDF* could be transformed and transmitted into off-gas during thermal treatment of spent LIBs, causing reactor corrosion and air pollution. Nevertheless, this method is worth studying, even though few researches have focused on it. Therefore, in this work, we investigated it, considering not only the thermal behaviors of the cathode materials but also the fate of fluorine. It is expected that our results will offer practical support for the large-scale recycling of spent LIBs.

Materials and methods

Materials

The spent LIBs were collected locally from mobile phone service providers. Prior to usage, they were discharged using NaCl solution to mitigate the potential risk of short circuiting or LIBs blasts. After drying, the discharged batteries were dismantled manually, and the metallic shell, organic separators, cathode, and anode were separated. The recovered cathodes were crushed and used as raw material for the experiments. In this study, the binding agent used for cathode was *PVDF*. During the LIBs preparation, *PVDF*, conductive agent acetylene black, and lithium cobalt oxide were generally stirred and mixed in a solvent *N*-methyl-2-pyrrolidone to form a uniform positive electrode slurry. The slurry was coated on a positive electrode current collector aluminum foil and dried and cold pressed to obtain a positive electrode plate.

Experimental methods

The online testing of evolved products during cathode thermal pretreatment was performed using a TG-FTIR-GC/MS (TGIRGCMS∗/TGA8000∗, PerkinElmer) coupled system. During analysis, approximately 2 mg of samples was heated from 30 to 1000 °C at a heating rate of 15 K min^{-1} with a flow rate of 50 mL min^{-1} for helium. Each test was repeated three times. The coupling systems between TG-FTIR-GC/MS were heated to prevent the condensation of volatile products.

Results and discussion

TG analysis

The thermogravimetric (TG) and derivative thermogravimetric (DTG) profiles of the cathode materials are displayed in Fig. 1. It can be seen that the cathode decomposition displayed a three-stage process, consistent with the previous reports (Zhang et al. 2014; Zhang et al. 2018a; Zhang et al. 2018b). There were two significant mass losses of 0.69% and 1.64% throughout the temperature ranges of 30–487 °C and 30–628 °C, respectively. The temperatures of maximum mass loss rate were determined as 470 °C and 599 °C, respectively. The mass loss in the initial stage was mainly attributed to the decomposition of *PVDF*, which was comparable to the reported decomposition temperature of 450–550 °C (Cao et al. 2016; Kar et al. 2015; Ma et al. 2012; Ouyang et al. 2015; Rathore et al. 2019). The loss in the second stage was mainly caused by the acetylene black oxidization (Cho et al. 2013; Nie et al. 2015). Cho et al. (2013) reported an exothermic peak of 604 °C for acetylene black decomposition. The loss in the last stage was attributed to the decomposition of lithium cobalt oxide (Antolini and Ferretti 1995; Zhang et al. 2014). From

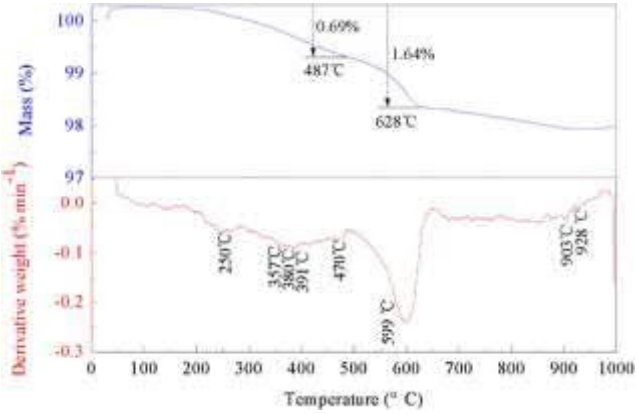

Fig. 1 TG-DTG profiles of cathode thermal treatment

the TG-DTG profiles, the optimal temperature for detaching cathode from Al foil was found to be approximately 650 °C.

Fourier transform infrared analysis

The 3D Fourier transform infrared (FTIR) spectra of the gas phase during the decomposition of cathode material are shown in Fig. 2. According to the y-axis (temperature) and z-axis (absorbance), the cathode decomposed vigorously, and more gaseous products were released in the temperature range of 550–1000 °C. From the perspective of the x-axis (wavenumbers) and the z-axis (absorbance), it can be observed that the absorbance peaks of evolved products were mainly located at 2000–2500 cm^{-1} (confirmed by Fig. 3). In addition, minor absorbances at 1500–2000 cm^{-1} and 3500–4000 cm^{-1} were also detected.

In order to probe the evolution of volatilized products, major signals from the gas phase spectra changes with respect to temperature were separated from the 3D spectra. In Fig. 4, the major peaks at 669, 2322, and 2360 cm^{-1} were attributed to the C–O bonds from CO_2 (Escribano et al. 2013; Yao et al. 2018; Yu et al. 2019). Minor peaks located at 1340 cm^{-1} were attributed to the C–F stretching vibration (Danilich et al. 1995; Mann et al. 1954). The bands at 1510 and 3739 cm^{-1} corresponded to the bending mode of H_2O. The release of CO_2 increased as temperatures increased from 195 to 928 °C. However, the release of H_2O showed a decreasing trend when the temperature increased to above 599 °C. The release of fluoride derivatives also exhibited a decreasing trend. They were not detected after temperatures increased to above 470 °C.

MS analysis

The simultaneous evolution of several volatile compounds having similar chemical structures did not allow the identification of single species by FTIR analysis, and thus MS analysis was adopted, to ensure the identification of specific products (Kai et al. 2017). First, a preliminary scan was carried out to identify the prominent ions with m/z in the range of 18 to 132 (see Fig. 5). Then, the main ionized fragments were tracked using multiple ion detection (MID) mode. Signals from m/z 12, 28, 44, 114, and 132 accounted for the evolution of small molecules H_2O, CO, CO_2, difluorobenzene ($C_6H_4F_2$, DFB), and trifluorobenze ($C_6H_3F_3$, TFB), respectively. Consistent with the DTG results, more gaseous products evolved in the temperature range of 350–650 °C. Signals at m/z 18, 28, and 44 revealed that the release of H_2O, CO, and CO_2 showed a three-stage process in the temperature ranges of 300–500 °C, 500–700 °C, and 700–900 °C, respectively. The release of H_2O and CO displayed a similar trend, with larger releasing intensity at the first two stages. However, the evolution of CO_2 showed a distinctive trend, with the largest release

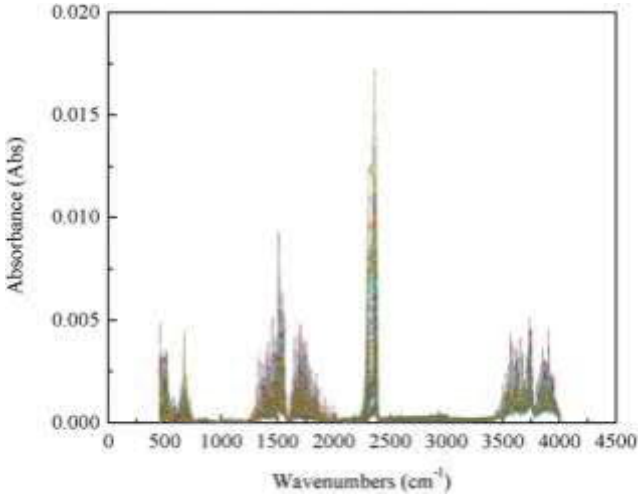

Fig. 3 2D infrared spectrum of evolved products for cathode thermal treatment

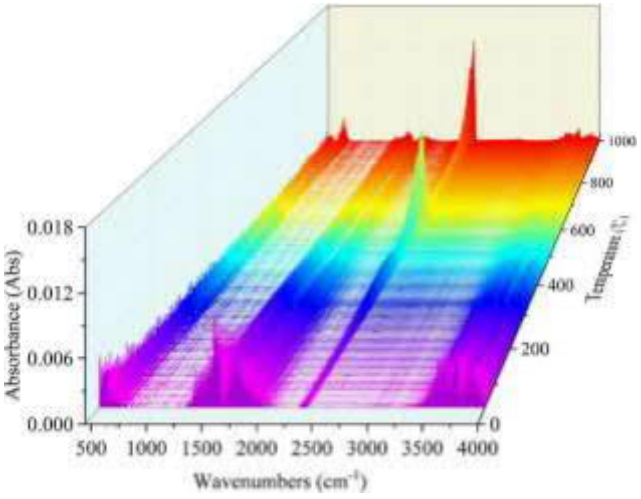

Fig. 2 3D infrared spectrum of evolved products for cathode thermal treatment

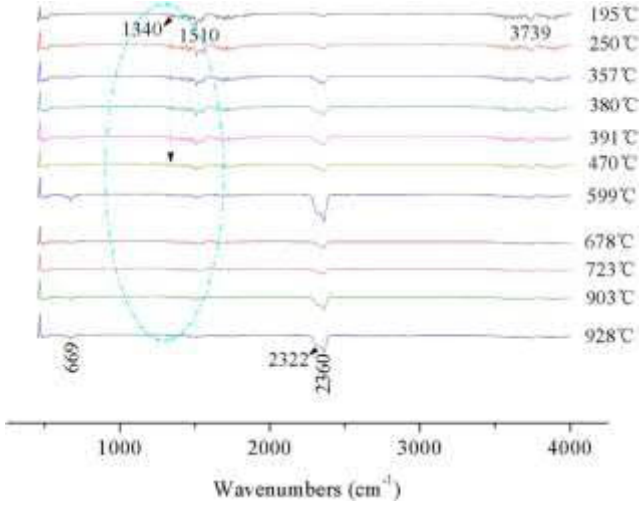

Fig. 4 FTIR spectra of volatilized products in cathode material thermal treatment

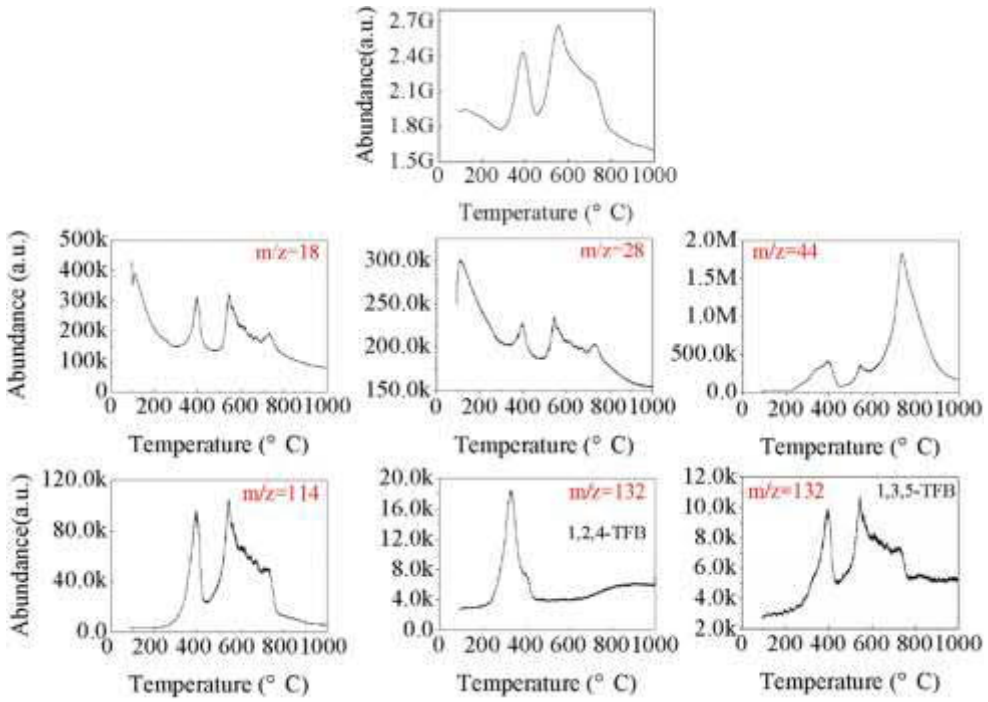

Fig. 5 Ion abundance distributions of evolved products along with temperatures

intensity at the third stage. Its release intensity was also larger than that of either H_2O or CO. This was consis- tent with the FTIR analysis in Fig. 4. In addition, fluo- rinated derivatives from the decomposition of *PVDF* were also detected, which was consistent with the FTIR analysis. Ion signals from m/z 114 and 132 indi- cated the evolution of 1,4-difluorobenzene ($C_6H_4F_2$, 1,4- DFB), 1,2,4-trifluorobenzene (1,2,4-TFB), and 1,3,5- trifluorobenzene (1,3,5-TFB). The release of 1,4-DFB and 1,3,5-TFB displayed a similar trend, with larger releasing intensity at the first two stages. However, the release of 1,2,4-TFB showed a different trend, with the release mainly focused at the temperature range of 300− 400 °C. The release intensities of 1,2,4-TFB and 1,3,5- TFB were comparable, although smaller than that of 1,4-DFB. The occurrence of fluorinated derivatives, such as 1,4-DFB, 1,2,4-TFB, and 1,3,5-TFB, were also detected in the pyrolysis of pure PVDF, although they were not identical due to differences in the temperature and sample characteristics. Choi and Kim (2012) re- vealed that the major products of *PVDF* pyrolysis were vinylidene fluoride (VDF), 1,3,5-TFB, 1,4-DFB, 1,2,4- TFB, and 1,3,3,5,5-pentafluorocyclohexene. O'Shea et al. (1990) reported that increasing pyrolysis tempera- ture resulted in a complex degradation process and a pyrolytic residue made up of largely aliphatic and fluoro-aromatic structures. The report of Zulfiqar et al. (1994) also indicated that the major degraded products of *PVDF* were HF, VDF, and $C_4H_3F_3$.

Conclusions

The thermogravimetric analysis indicated that the cathode de-composition displayed a three-stage process. There were two significant mass losses of 0.69% and 1.64% throughout the temperature ranges of 30−487 °C and 30−628 °C, respectively, and the temperatures of maximum mass loss rate were located at 470 °C and 599 °C, respectively. The FTIR analysis indicated that the release of CO_2 increased as temperatures rose from 195 to 928 °C. However, the release of H_2O showed a decreasing trend when the temperature increased to above 599 °C. The release of fluoride derivatives also exhibited a decreasing trend, and they were not detected after tempera-tures increased to above 470 °C. The GC-MS analysis re-vealed that more gaseous products were evolved in the tem-perature range of 350−650 °C. The release of H_2O and CO displayed a similar trend, with larger releasing intensity at the first two stages. However, the evolution of CO_2 showed a distinctive trend, with the largest release intensity at the third stage. Its release intensity was also larger than that of H_2O or CO. The release of 1,4-DFB and 1,3,5-TFB displayed a sim-ilar trend, with larger releasing intensity at the first two stages. However, the release of 1,2,4-TFB showed a different trend, and the release was mainly focused at the temperature range of 300−400 °C. The release intensities of 1,2,4-TFB and 1,3,5-TFB were comparable, although smaller than that of 1,4-DFB.

Funding information This work was financially supported by the Zhejiang Provincial Natural Science Foundation of China (Grant no. LY19B070008).

References

Antolini E, Ferretti M (1995) Synthesis and thermal stability of $LiCoO_2$. J Solid State Chem 117(1):1–7

Cao Y, Liang M, Liu Z, Wu Y, Xiong X, Li C, Wang X, Jiang N, Yu J, Lin CT (2016) Enhanced thermal conductivity for poly (vinylidene fluoride) composites with nano-carbon fillers. RSC Adv 6(72):68357–68362

Chen X, Zhou T (2014) Hydrometallurgical process for the recovery of metal values from spent lithium-ion batteries in citric acid media. Waste Manag Res 32(11):1083–1093

Cheng S, Qiao Y, Huang J, Wang W, Wang Z, Yu Y, Xu M (2019) Effects of Ca and Na acetates on nitrogen transformation during sewage sludge pyrolysis. Proc Combust Inst 37(3):2715–2722

Cho T, Han C, Jun Y et al (2013) Formation of artificial pores in nano-TiO_2 photo-electrode films using acetylene-black for high-efficiency, dye-sensitized solar cells. Sci Rep 3:1496

Choi S, Kim Y (2012) Microstructural analysis of poly (vinylidene fluoride) using benzene derivative pyrolysis products. J Anal Appl Pyrolysis 96:16–23

Danilich MJ, Burton DJ, Marchant RE (1995) Infrared study of perfluorovinylphosphonic acid, perfluoroallylphosphonic acid, and pentafluoroallyldiethylphosphonate. Vib Spectrosc 9(3):229–234

Duan C, Li F, Yang M et al (2018) Rapid synthesis of hierarchically structured multifunctional metal-organic zeolites with enhanced volatile organic compounds adsorption capacity. Ind Eng Chem Res 57(45):15385–15394

Escribano RM, Caro GMM, Cruz-Diaz GA et al (2013) Crystallization of CO_2 ice and the absence of amorphous CO_2 ice in space. Proc Natl Acad Sci 110(32):12899–12904

Gao W, Liu C, Cao H, Zheng X, Lin X, Wang H, Zhang Y, Sun Z (2018) Comprehensive evaluation on effective leaching of critical metals from spent lithium-ion batteries. Waste Manag 75:477–485

He Y, Zhang T, Wang F, Zhang G, Zhang W, Wang J (2017) Recovery of $LiCoO_2$ and graphite from spent lithium-ion batteries by Fenton reagent-assisted flotation. J Clean Prod 143:319–325

Kai X, Li R, Yang T, Shen S, Ji Q, Zhang T (2017) Study on the co-pyrolysis of rice straw and high density polyethylene blends using TG-FTIR-MS. Energy Convers Manag 146:20–33

Kar E, Bose N, Das S, Mukherjee N, Mukherjee S (2015) Enhancement of electroactive β phase crystallization and dielectric constant of PVDF by incorporating GeO_2 and SiO_2 nanoparticles. Phys Chem Chem Phys 17(35):22784–22798

Liu C, Lin J, Cao H, Zhang Y, Sun Z (2019) Recycling of spent lithium-ion batteries in view of lithium recovery: a critical review. J Clean Prod 228:801–813

Ma J, Haque RI, Larsen RM (2012) Crystallization and mechanical properties of functionalized single-walled carbon nanotubes/polyvinylidene fluoride composites. J Reinf Plast Compos 31(21):1417–1425

Mann DE, Acquista N, Plyler EK (1954) Vibrational spectrum of Bromotrifluoroethylene. J Chem Phys 22(7):1199–1202

Natarajan S, Aravindan V (2018) Recycling strategies for spent Li-ion battery mixed cathodes. ACS Energy Letters 3(9):2101–2103

Nie H, Xu L, Song D, Song J, Shi X, Wang X, Zhang L, Yuan Z (2015) $LiCoO_2$: recycling from spent batteries and regeneration with solid state synthesis. Green Chem 17(2):1276–1280

O'Shea ML, Morterra C, Low M (1990) Spectroscopic studies of carbons. XVII Pyrolysis of polyvinylidene fluoride. Mater Chem Phys 26(2):193–209

Ouyang Z, Chen E, Wu T (2015) Thermal stability and magnetic properties of polyvinylidene fluoride/magnetite nanocomposites. Materials 8(7):4553–4564

Qi W, Liu G, He C, Liu S, Lu S, Yue J, Wang Q, Wang Z, Yuan Z, Hu J (2019) An efficient magnetic carbon-based solid acid treatment for corncob saccharification with high selectivity for xylose and enhanced enzymatic digestibility. Green Chem 21(6):1292–1304

Rathore S, Madhav H, Jaiswar G (2019) Efficient nano-filler for the phase transformation in polyvinylidene fluoride nanocomposites by using nanoparticles of stannous sulfate. Mater Res Innov 23(4):183–190

Sun C, Xu L, Chen X, Qiu T, Zhou T (2018) Sustainable recovery of valuable metals from spent lithium-ion batteries using DL-malic acid: leaching and kinetics aspect. Waste Manag Res 36(2):113–120

Tran MK, Rodrigues MF, Kato K et al (2019) Deep eutectic solvents for cathode recycling of Li-ion batteries. Nat Energy 4(4):339–345

Wang F, Zhang T, He Y, Zhao Y, Wang S, Zhang G, Zhang Y, Feng Y (2018) Recovery of valuable materials from spent lithium-ion batteries by mechanical separation and thermal treatment. J Clean Prod 185:646–652

Wang M, Tan Q, Liu L, Li J (2019a) A low-toxicity and high-efficiency deep eutectic solvent for the separation of aluminum foil and cathode materials from spent lithium-ion batteries. J Hazard Mater 380:120846

Wang M, Tan Q, Liu L, Li J (2019b) Efficient separation of aluminum foil and cathode materials from spent lithium-ion batteries using a low-temperature molten salt. ACS Sustain Chem Eng 7:8287–8294

Winslow KM, Laux SJ, Townsend TG (2018) A review on the growing concern and potential management strategies of waste lithium-ion batteries. Resour Conserv Recycl 129:263–277

Xiao J, Li J, Xu Z (2017) Novel approach for in situ recovery of lithium carbonate from spent lithium ion batteries using vacuum metallurgy. Environmental Science & Technology 51(20):11960–11966

Xiao J, Li J, Xu Z (2020) Challenges to future development of spent lithium ion batteries recovery from environmental and technological perspectives. Environmental Science & Technology 54(1):9–25

Yao J, Chen J, Shen K, Li Y (2018) Phase-controllable synthesis of MOF-templated maghemite-carbonaceous composites for efficient photocatalytic hydrogen production. J Mater Chem A 6(8):3571–3582

Yu S, Su W, Wu D, Yao Z, Liu J, Tang J, Wu W (2019) Thermal treatment of flame retardant plastics: a case study on a waste TV plastic shell sample. Sci Total Environ 675:651–657

Zeng X, Li J (2014) Innovative application of ionic liquid to separate Al and cathode materials from spent high-power lithium-ion batteries. J Hazard Mater 271:50–56

Zhang Z, He W, Li G et al (2014) Ultrasound-assisted hydrothermal renovation of $LiCoO_2$ from the cathode of spent lithium-ion batteries. Int J Electrochem Sci 9:3691–3700

Zhang G, He Y, Feng Y, Wang H, Zhang T, Xie W, Zhu X (2018a) Enhancement in liberation of electrode materials derived from spent lithium-ion battery by pyrolysis. J Clean Prod 199:62–68

Zhang G, He Y, Feng Y, Wang H, Zhu X (2018b) Pyrolysis-ultrasonic-assisted flotation technology for recovering graphite and $LiCoO_2$ from spent lithium-ion batteries. ACS Sustain Chem Eng 6(8):10896–10904

Zhang W, Xu C, He W, Li G, Huang J (2018c) A review on management of spent lithium ion batteries and strategy for resource recycling of all components from them. Waste Manag Res 36(2):99–112

Zhang X, Li L, Fan E, Xue Q, Bian Y, Wu F, Chen R (2018d) Toward sustainable and systematic recycling of spent rechargeable batteries. Chem Soc Rev 47(19):7239–7302

Zhang G, Du Z, He Y et al (2019) A sustainable process for the recovery of anode and cathode materials derived from spent lithium-ion batteries. Sustainability 11(8):2363

Zhao S, Li G, He W, et al. (2019) Recovery methods and regulation status of waste lithium-ion batteries in China: a mini review. Waste Manag Res DOI: https://doi.org/10.1177/0734242X19857130, 2019-06-27

Zulfiqar S, Zulfiqar M, Rizvi M, Munir A, McNeill IC (1994) Study of the thermal degradation of polychlorotrifluoroethylene, poly (vinylidene fluoride) and copolymers of chlorotrifluoroethylene and vinylidene fluoride. Polym Degrad Stab 43(3):423–430